Journal of Environmental Chemical Engineering 9 (2021) 105480

Contents lists available at ScienceDirect

Journal of Environmental Chemical Engineering

journal homepage: www.elsevier.com/locate/jece

Synergistic effect of NS co-doped TiO_2 adsorbent for removal of cationic dyes

Ruhma Rashid [a,b], Iqrash Shafiq [b], Muhammad Javid Iqbal [a], Maira Shabir [b], Parveen Akhter [c], Muhammad Haris Hamayun [b], Ashfaq Ahmed [b], Murid Hussain [b,*]

[a] Department of Chemistry, COMSATS University Islamabad, Lahore Campus, Defence Road, Off Raiwind Road, Lahore, Pakistan
[b] Department of Chemical Engineering, COMSATS University Islamabad, Lahore Campus, Defence Road, Off Raiwind Road, Lahore, Pakistan
[c] Department of Chemistry, The University of Lahore, 1-km Defence Road, Off Raiwind Road, Lahore, Pakistan

ARTICLE INFO

Editor: Dr. Zhang Xiwang

Keywords:
Adsorption
Dye removal
NS co-doped TiO_2
Parametric study

ABSTRACT

Removal of dyes from wastewater specially from textile effluents has been given considerable attention in the last few decades, not only for their health issues but also potential toxicity. Over the former few eras, TiO_2 based adsorbents have drawn worldwide attention as an efficient adsorbent for wastewater treatment due to their versatile physio-chemical characteristics. This paper outlined the synthesis of nitrogen and sulfur co-doped TiO_2 (NS/TiO_2) nanostructures and highlighted their applications in the removal of dyes, including methylene blue (MB), methyl orange (MO) and methyl red (MR). The nanostructures were characterized by using scanning electron microscopy (SEM), X-Ray Diffraction pattern (XRD), Brunauer-Emmett-Teller measurements (BET), Fourier transform infrared spectroscopy (FTIR) and Raman spectroscopy. Batch experiments of adsorption were carried out by varying solution pH, adsorbent dose, initial dye concentration and contact time. The results revealed that dye adsorption capacity increased with increased adsorbent dosage up to 0.06 g, solution pH from 1 to 14 and contact time from 20 to 140 min. However, the adsorption capacity decreases with increase in the initial dye concentration. The experimental data were analyzed by the Langmuir and Freundlich adsorption isotherms. NS/TiO_2 adsorbent exhibited a high affinity towards organic dyes due to the heterogeneous sorption capacity. The NS/TiO_2 adsorbent showed 99.4% removal efficiency for MB, 98% for MO and 96% for MR. The adsorbent could be regenerated in an acidic medium for MB and a basic medium for MO and MR with good activity, even after three repeated cycles.

1. Introduction

The faster evolution of industrial events united with development in science and technology advances living standards, leading to supportable financial growth and universal competitiveness [1]. The expense of this rapid development is a natural ailment with the massive pollution problem [2–4]. Water pollution is considered one of the extreme concerns that the biosphere confronts today [5,6]. The created dye toxins from wastewater discharged from industrial effluents comprise various sorts of inorganic and organic contaminants, which is a threat not only for human health but also for the surrounding environment [7]. Globally, ejection of 280,000 tons/year of textile wastes are expected to be discharged extensively contaminating the groundwater [8].

Dyes are fundamentally nonbiodegradable chemical composites that can link themselves to fabrics or surfaces to give colour. Typical examples include methyl orange, methyl red, congo red, methylene blue, acid yellow, etc. [9,10]. Synthetic dyes are extensively used in various unconventional technology fields, i.e., in numerous textile industry courses, rubber, plastic, cosmetics, paper and leather tanning, dye manufacturing and printing [8,11]. Approximately more than 100 tonnes per year of colours are liquidated into watercourses [12]. It is problematic to eliminate dyes from the wastewater because most of the dyes are cancer-causing and typically produce poisonous organic complexes when they are biologically degraded [8]. Moreover, exposure of

Abbreviations: NS/TiO_2, Nitrogen and Sulfur co-doped TiO_2; MB, Methylene blue; MO, Methyl orange; MR, Methyl red; SEM, Scanning electron microscopy; XRD, X-Ray diffraction pattern; BET, Brunauer-Emmett-Teller measurements; FTIR, Fourier transform infrared spectroscopy; TTIP, Titanium tetraisopropoxide; IPA, Isopropyl alcohol; DI, Deionized; HCl, Hydrochloric acid; NaOH, Sodium hydroxide.

* Corresponding author.
E-mail address: drmhussain@cuilahore.edu.pk (M. Hussain).

https://doi.org/10.1016/j.jece.2021.105480
Received 26 January 2021; Received in revised form 27 March 2021; Accepted 7 April 2021
Available online 12 April 2021
2213-3437/

marine species to the dyes is devastating as it decreases the dissolved oxygen. Henceforth, there is a need to develop a technique to eliminate dyes from manufacturing waste before it is liquidated into the surrounding environment [13].

In recent centuries, the incredible struggle has been made in order to grow progressive technology for the removal of pollutants from industrial wastewater [14], as population is increased demand for purified drinking water has also been increased [15]. In this framework, different chemical, physical, and biological approaches have been implemented including, solvent extraction, membrane filtration, electrochemical treatment, ozonation, advanced oxidation and adsorption process to remove pollutants and dyes from industrial wastewater [16]. Nonetheless, each of the mentioned techniques, except adsorption, possesses muddled issues comprising higher capital cost, lesser efficiency, high cost of maintenance and excessive sludge production make them inappropriate economically [17].

Adsorption is a promising technology owing to its easy and simple handling, higher proficiency, minimal cost requirements and excellent reproducibility [15]. The adsorption process is ordered into two classifications, i.e., physical and chemical adsorption, in the light of interactions type possess by adsorbate and adsorbent molecules [18]. Besides, the process is reversible in most cases, and hence, the adsorbents can be regenerated quickly and reused frequently [19]. These properties make the adsorption process more economical. Moreover, the accessibility of a wide range of adsorbents makes the adsorption process versatile to suit exact needs [20]. There are various factors, including surface area, particle size, adsorbate-adsorbent interaction, adsorbent to adsorbate ratio, pH, temperature, contact time and concentration, which are liable to remove pollutants effectively [21,22]. In recent times, nanotechnology is considered quite possibly a strong trend in material sciences. The word of nanotechnology denotes to the materials that at least one of their dimension (thickness, width and length) is in the range of nanometers (1–100 nm) [23]. High reactivity, high adsorption-desorption capacity and large surface area are fundamental attributes of nanomaterials [23–25].

Many studies have reported the applications of TiO_2 as an adsorbent [26,27]. Additionally, some works have been explored to investigate the water molecules efficiency adsorbed on the titania surface [28,29]. TiO_2 NPs are very trendy in the fields of the material sciences [30,31]. Due to its bulk assets and widespread usages in various areas, titania has been exploited as an adsorbent many times [32]. TiO_2 nanostructures show high adsorption potential for removing toxic dyes due to their high stability, nontoxicity, corrosion resistance and inexpensiveness [33]. Doping different materials onto the TiO_2 surface is an operative approach to magnify its adsorption capacity and separation efficiency [34]. In this framework, Raveendra et al. [35] have reported nano $ZnTiO_2$ ceramic synthesis as an adsorbent and explore its removal efficiency for azo dyes from wastewater. Likewise, Zhao et al. [36] synthesized carbon-doped TiO_2 adsorbent for the removal of rhodamine B and MO up to 98% in 20 min. Baig et al. [32] reported the synthesis of polypyrrole coated TiO_2 as an adsorbent for efficient removal of anionic dye (congo red) up to 98.75%.

In this study, the NS/TiO_2 has been examined for the first time as an adsorbent. The laboratory synthesized TiO_2 nanoparticles and NS/TiO_2 nanocomposites were characterized by SEM, XRD, BET, FTIR and Raman spectroscopy and the adsorption capability was studied by UV-Vis spectroscopy. Methylene blue (MB), methyl red (MR) and methyl orange (MO) were investigated as model dyes in this work. The adsorption isotherms for the adsorption of MB dye were plotted and discussed. The influence of different operating parameters such as adsorbent dosage, solution pH, initial dye concentration and interaction time on adsorption was also evaluated and their optimized adsorbent dosage, pH and contact time with maximum adsorption capacity is presented. The superlative results, regeneration and reusability of the as-synthesized NS/TiO_2 nanocomposite have confirmed its suitability as an adsorbent for removing dyes from wastewater.

2. Experimental

2.1. Materials

All the chemicals used for the synthesis of adsorbents were analytical-grade reagents and used without additional purification. These chemicals include Titanium tetraisopropoxide (TTIP, $C_{12}H_{28}O_4Ti$, 97%, DAEJUNG CHEMICALS & METALS CO. LTD, Korea), Isopropyl alcohol (IPA, C_3H_8O, 99%, ACS reagent, Riedel-de Haen, Germany), Thiourea (CH_4N_2S, 99.9%, ACS reagent, SIGMA-ALDRICH, Germany), Hydrochloric acid (HCl, 37%, CARLO ERBA Reagents, Spain) and Sodium hydroxide (NaOH, 98.9%, Fisher scientific, England).

2.2. Synthesis of adsorbents

Undoped TiO_2 and NS/TiO_2 samples were synthesized by the sol-gel and calcination process, respectively. Undoped TiO_2 was prepared by the sol-gel method in which TTIP was used as a precursor. 10 ml of TTIP was dissolved in 10 ml of IPA with constant stirring for 5–10 min. After stirring, 66.84 g of DI water was added to the existing solution dropwise, followed by the addition of 0.0169 g of HCl to maintain pH at 4. Then the solution was stirred for two hours at room temperature. White precipitates were formed after a specified time which was filtered by vacuum filtration. Filtered precipitates were dried in an oven at 85° C for four hours and calcined in Muffle Furnace at 400° C for two hours.

In the synthesis process of NS/TiO_2, 0.0375 mol of TTIP was dissolved in 20 ml of IPA under continuous stirring (Fig. 1). During the stirring of TTIP and IPA, 6 ml of deionized water containing 1.42 g of thiourea (precursor of nitrogen and sulfur) was added dropwise and left for two hours stirring at room temperature. After that, the material was dried overnight in the drying oven at 80° C. The as-synthesized sample was then calcined at 550° C for two hours in a muffle furnace [37].

2.3. Adsorption experiment

An adsorption experiment was performed to determine the adsorption of MB on the as-synthesized adsorbents. An aqueous solution of 30 ppm MB was prepared. The effects of initial concentration, the adsorbent dosage, solution pH and contact time were investigated. Initially, the adsorption experiment was carried out by adding 0.03, 0.06 and 0.09 g of undoped TiO_2 and NS/TiO_2 with 20 ml solution in a water bath shaker at 100 rpm for 100 min at room temperature. After a certain time, the supernatant was filtered out and measured by a UV–vis spectrophotometer at a wavelength of 664 nm [38]. The MB dye concentration was investigated by drawing a calibration curve between the solution concentration and the corresponding absorbance value. The MB dye adsorption was determined by following the mass balance Eq. (1)

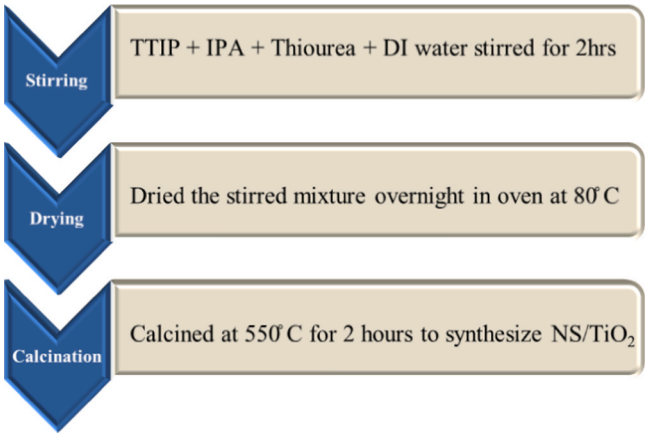

Fig. 1. Synthesis process of NS/TiO_2.

[16,39]:

$$\% \text{ Adsorption} = C_o - C_e/C_o \times 100 \quad (1)$$

Where C_o is the initial dye concentration and C_e is the dye concentration at equilibrium after adsorption. The same procedure was followed by MB adsorption for different pH (1−14), concentration (10–40 mg/L) and contact time (20–140 min).

Pure TiO_2 and NS/TiO_2 investigated the adsorption experiment for MO and MR at concentrations of 30 ppm, pH of 4–5, adsorbent dose of 0.06 g and contact time of 100 min at room temperature. After a particular time, the supernatant was filtered out and measured by a UV-Vis spectrophotometer at a wavelength of 464 nm and 520 nm for MO and MR, respectively. The adsorption for the removal of dyes was pre-meditated by Eq. (1).

2.4. Adsorption isotherms

The adsorption isotherm models describe the adsorption of circulated molecules between the solid and liquid interphases. A batch experiment on MB dye was carried out with a 0.06 g dosage of NS/TiO_2 adsorbent, initial concentration of dye was 10–50 ppm and the pH of the solution was retained 10 using 0.1 M NaOH and 0.1 M HCl solution. The different concentration solutions were positioned in the water bath shaker at 100 rpm for four hours at 298 K. The aliquots for MB were examined in UV–vis Spectrometer at the wavelength of 664 nm [10].

2.5. Regeneration

The regeneration of the adsorbed dye from NS/TiO_2 adsorbent was carried out at room temperature with pH 4 for MB and pH 10 for MO and MR, as convening to the pH effect on adsorption and surface charges, no fascinating desirability between the NS/TiO_2 and the dye occurs at this pH and hence the ability of the adsorbent to adsorb the dye molecules are insignificant. The dye retrieval experiment showed almost complete desorption of adsorbed dye after 30 min. After desorption, the adsorbent was then collected by filtration, multiple times washed with deionized water and kept drying at 60 ◦C for one hour.

2.6. Characterization

Scanning Electron Microscopy (SEM - Philips XL 30 FED) analyzed the morphology and surface analysis of adsorbents. The crystalline structre of the samples was investigated by XRD pattern. Brunauer-Emmett-Teller measurements investigated surface area, pore volume and pore size by the nitrogen adsorption-desorption method (BET - Micromeritics Tristar II) at 77 K. Fourier Transform Infrared Spectroscopy was performed on (FTIR - Nicolet 20 SX) with a wavenumber of 400–4000 cm^{-1} and Raman Spectroscopy (RS) analyzed the functional group present at the adsorbent surface using (Via Raman Microscope) for 100–1000 cm^{-1} range for the exposure for 10 s

3. Results and discussion

3.1. Characterization of adsorbents

To examine the as-synthesized adsorbent morphology, SEM images for the composite material were taken at room temperature. The small irregular shaped particles having an apparent size of a few nm for NS/TiO_2 were observed, as shown in Fig. 2. Single-particle accumulations of NS in TiO_2 nanoparticles exhibited arbitrary shapes with a narrow size distribution. The composite material size is smaller than the pure TiO_2 crystallite size previously reported in the literature [40,41].

The XRD analyses of commercial TiO_2, synthesized TiO_2 and NS/TiO_2 were carried out from 5° to 90° as shown in Fig. 3. The standard crystallite size (D) of the samples was calculated by the Scherrer's Eq. (2)

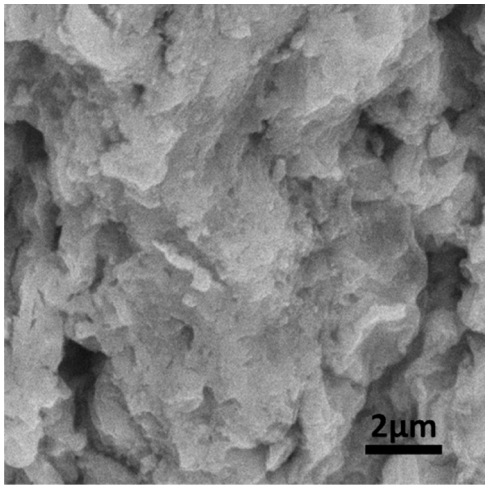

Fig. 2. SEM micrographs of the as-synthesized NS/TiO_2.

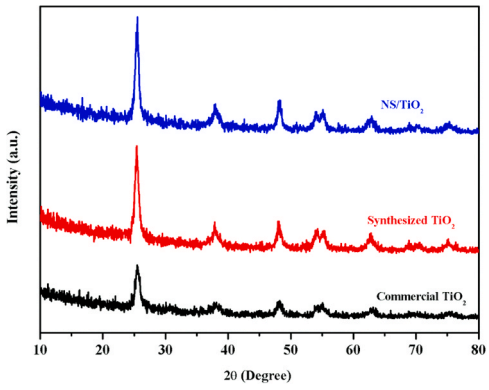

Fig. 3. XRD pattern of commercial TiO_2, synthesized TiO_2 and NS/TiO_2.

[40].

$$D = k\lambda / \beta \cos \theta \quad (2)$$

Where k is Scherrer constant, λ is X- ray radiation wavelength, β is XRD peak width at half peak height and θ is the diffraction angle [42].

All the characteristic diffraction peaks at angle 25.78°, 37.87°, 48.1° and 55° can be allotted to commercial TiO_2, synthesized TiO_2 and NS/TiO_2. The regular crystallite size of all the samples calculated using the Scherer equation are 14.1, 10.5 and 5.1 nm, respectively. The crystallite size decreases in the following order: commercial TiO_2 > synthesized TiO_2 > NS/TiO_2. Moreover, the doping of nitrogen and sulfur causes the decrease in crystallite size of samples. It can be assumed that presence of the doping species inhibits the growth of crystallite structure, similarly as impurities and additives suppress growth of grain during sintering [43].

The effect of pore size, pore volume and specific surface area of TiO_2 is essential in the adsorption process. The primary objective of synthesizing NS/TiO_2 was to generate high pore volume and surface area [44]. Table 1 shows the BET measurements of the co-doped TiO_2. It is determined that the surface area of NS/TiO_2 is higher than commercial

Table 1
BET measurements of NS/TiO_2.

Material	Surface area (m^2/g)	Pore volume (cm^3/g)	Pore size (nm)	Nanoparticle size (nm)
NS/TiO_2	54.4653	0.00133	1.979	110.1618

titania, offering the best available surface area for the adsorption of dyes after doping. Co-doped titania also has a pore size of 1.98 nm and pore volume of 0.00133 cm^3/g. This porosity provides void space than the un-doped material. The sample with a rough surface (as shown in the SEM image) and characteristic porosity with more adsorption capacity. Alternatively, the increased surface area of NS/TiO_2 can improve the surface activity and surface reaction of composite material [45,46].

The FTIR spectrum of TiO_2 presented various characteristic bands, as shown in Fig. 4. The absorption band at 3454.51 cm^{-1} represents stretching vibrations of the O–H bond, indicating the moisture content. The sharp band at 690.52 cm^{-1} is allotted to Ti–O stretching, representing the characteristic band of TiO_2 nanoparticles [47]. The bands between 3400 and 3500 cm^{-1} correspond to N–H stretching and a small band appearing at 1658.72 cm^{-1} is detected as N–O bending vibrations [48]. The band at 1058.30 cm^{-1} represent the Ti–O–S bonding, which indicates the incorporation of sulfur in TiO_2. The band at 1188.71 cm^{-1} indicates the S–O vibrations and, more precisely, to a typical frequency of SO_4^{-2} ions [49].

Raman spectroscopy is a prevailing technique for the characterization of microstructural and surface information of various oxides. The Raman spectroscopy was also applied to analyze the species at the material surface. Fig. 5. exhibits a strong band at 147 cm^{-1} and the three other bands at 641, 521 and 400 cm^{-1}. These bands typically analyze the characteristic peaks of titania [50].

Group theory forecasts that the typical TiO_2 has six Raman active modes: $A_{1\,g} + 2B_{1\,g} + 3E_g$. Moreover, a substantial redshift and a small full-width at 147 cm^{-1} is observed for the N-TiO_2 sample. The decrease in peak broadening might be ascribed to the development of N and S doping [51]. It is estimated that the shifting of peak either to a higher or lower wavenumber takes place due to doping effect in NS/TiO_2 [52].

3.2. Adsorption results

3.2.1. Effect of adsorbent dose

The effect of dosage on adsorption of MB using conventional TiO_2 (commercial), synthesized TiO_2 and NS/TiO_2 was investigated at 0.03 g, 0.06 g and 0.09 g (C_o - 30 ppm; pH - 10; temperature - 298 K; agitation speed - 100 rpm; contact time - 100 min). The adsorption of MB was measured by UV–vis spectrometer at wavelength 664 nm.

It was detected that with an increase in the adsorbent quantity, removal of dye (MB) was enhanced at the initial stage as more active charge bearing sites were available for the adsorption. As the adsorption proceeds, at a specific adsorbent dosage, equilibrium is obtained and maximum adsorption is recorded at that point. Hence, after the saturation point, no further increase in adsorption was recorded, although the quantity of adsorbent increases. Fig. 6 represents the removal efficiency of conventional, synthesized and NS/TiO_2 at optimized adsorbent dosage. Maximum adsorption is obtained by conventional (89.6%), synthesized (92.2%) and NS/TiO_2 (95.9%) at 0.06 g, which confirms the best adsorbent dose for MB dye. Tanhaei et al. reported the same trend of adsorbent dosage for removing MB using chitosan/Al_2O_3/magnetite nanoparticles composite, supporting our results [53].

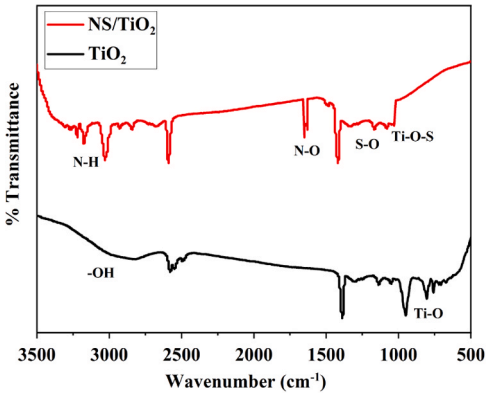

Fig. 4. FTIR pattern of the as-synthesized NS/TiO_2.

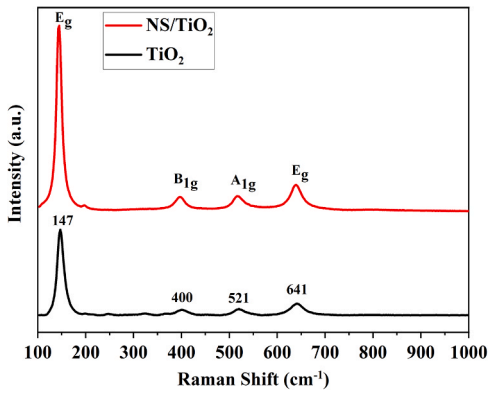

Fig. 5. Raman analysis of the as-synthesized NS/TiO_2.

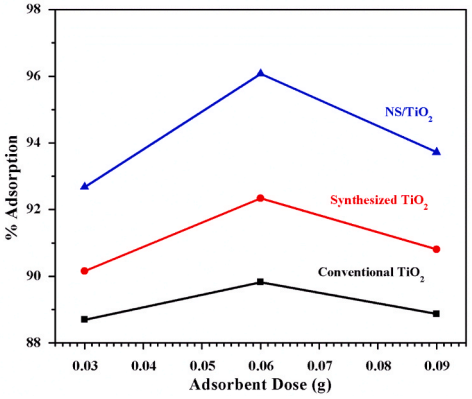

Fig. 6. Effect of the adsorbent dosage on the adsorption performance.

3.2.2. Effect of pH

The effect of pH on adsorption of MB using conventional TiO_2, synthesized TiO_2 and NS/TiO_2 was investigated at 1–14 (C_o - 30 ppm; adsorbent dose - 0.06 g; temperature - 298 K; agitation speed - 100 rpm; contact time - 100 min). It was observed that adsorption capacity increased with an increase in the solution pH value. At a low pH, TiO_2 adsorbents gain a positive charge at the surface. This positively charged surface of adsorbents creates electrostatic repulsion between adsorbent and MB cationic fragments, resulting in a reduction in adsorption capacity. At low pH, more H+ ions compete with MB, hence decreases the adsorption in acidic media. As the solution pH increases, the charge on the adsorbent surface became more negative because of deprotonation. At the same time, competition between H^+ and cationic dye molecules became less prominent. Resultantly, the adsorption capacity dramatically increased. Fig. 7 represents the removal efficiency of conventional, synthesized and NS/TiO_2 at optimized pH. Maximum adsorption is obtained by commercial (88%), synthesized (94.3%) and NS/TiO_2 (99.2%) at a pH of 10, confirming MB adsorption best pH value. Wang et al. reported the same trend for MB adsorption by using reduced graphene oxide/titania nanocomposites as an adsorbent that supports our results [38].

3.2.3. Effect of concentration

The effect of solution concentration on MB adsorption using conventional TiO_2, synthesized TiO_2 and NS/TiO_2 was investigated at 10, 20, 30 and 40 mg/L (adsorbent dose - 0.06 g; pH - 10; temperature - 298 K; agitation speed - 100 rpm; contact time - 100 min). It is observed

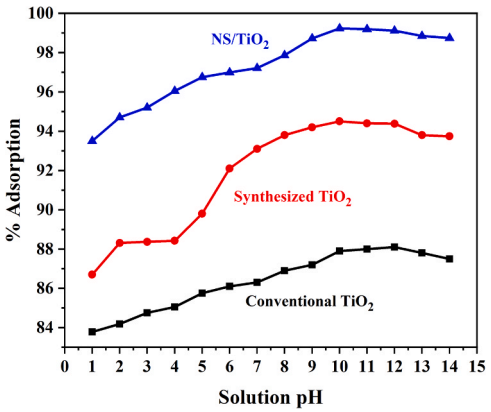

Fig. 7. Effect of the solution pH on the adsorption of MB dye.

that the initial dye concentration shows a significant impact on the adsorption capacity, which can urge the solute molecules to overwhelmed the mass transfer resistance amongst the solid and the liquid phases. It is clear from the Fig. 6 that adsorption decreases as the initial dye concentration increases. Fig. 8 represents the removal efficiency of commercial, synthesized and NS/TiO_2 at different concentrations. Maximum adsorption is obtained by commercial (87.5%), synthesized (94.4%) and NS/TiO_2 (99%) at 10 ppm for MB solution. Ramaraju et al. reported the same trend for the adsorption process at different initial concentrations using low-cost adsorbent from agricultural wastes, supporting our results [54].

3.2.4. *Effect of contact time*

The effect of time interval on MB adsorption using conventional TiO_2, synthesized TiO_2 and NS/TiO_2 was investigated at 20, 40, 60, 80, 100, 120 and 140 min (C_o - 30 ppm; adsorbent dose - 0.06 g; pH - 10; temperature - 298 K; agitation speed - 100 rpm). The results revealed that MB adsorption at the initial stage is very fast due to many free active sites for conventional, synthesized and NS/TiO_2. Over time, the adsorption process slows down so that the adsorption percentage becomes parallel to the x-axis, which is considered almost constant at 100 min Fig. 9 represents the removal efficiency of conventional, synthesized and co-doped titania at an optimized time. Maximum adsorption is obtained by commercial (87.7%), synthesized (91.8%) and NS/TiO_2 (99.4%) at 100 min, which confirms that it is optimized contact time. Naushad et al. reported the same contact time trend for MB adsorption using arginine modified activated carbon, supporting our results [39].

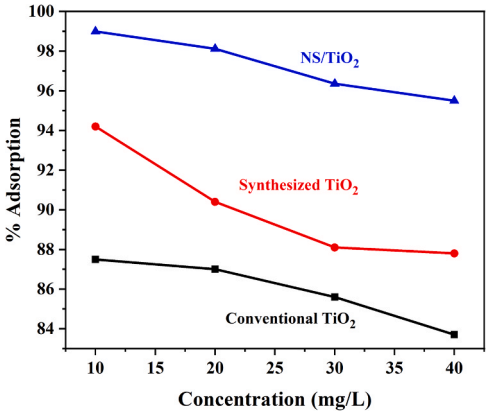

Fig. 8. Effect of the initial dye concentration on the adsorption performance.

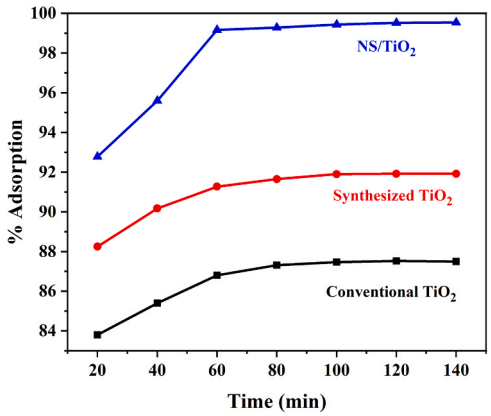

Fig. 9. The adsorption performance of different adsorbents over time under optimized conditions.

3.3. *Applications on MO and MR removal*

The effect of NS/TiO_2 on adsorption capacity of MB, MO and MR at optimized conditions (C_o - 30 ppm; pH – 10 (MB), pH – 4.5 (MO), pH – 5 (MR); temperature - 298 K; contact time – 140 min; agitation speed - 100 rpm) was observed. The adsorption of MB, MO, and MR was measured by UV–vis spectrometer at wavelength 664, 466 and 410 nm. It was estimated that NS/TiO_2 shows maximum adsorption for MB (99.4), MO (98.4) and MR (96.7). Hence, the maximum adsorption capacity was obtained for MB dye and thus, NS/TiO_2 is considered the best adsorbent for removing MB.

3.4. *Isotherm analysis*

The adsorption isotherm is substantial for explaining adsorbent interaction with adsorbate molecules to express the adsorption capacity. In the description of adsorption isotherms, adsorption equilibrium is considered a dynamic concept that explains that dye adsorption is equal to the rate of dye desorption. Hence, this equilibrium test delivers physio-chemical data for the feasibility of the adsorption process. The surface segment might be considered as a monolayer or might be a multilayer. Several adsorption isotherms are existing in the literature [55]. In this examination, Langmuir isotherm and Freundlich isotherm were utilized to signify MB dye's adsorption information onto as-synthesized NS/TiO_2 adsorbent.

The Langmuir isotherm is effective for monolayer adsorption on adsorbent surfaces with a limited number of indistinguishable sites [56]. According to this model, all the sites on the adsorbent surface are energetically equal. Once the molecules accumulate at a particular location, no further adsorption occurs at the adsorbent site [66]. The equation for Langmuir isotherm is expressed as Eq. (3).

$$C_e/q_e = C_e/q_m + 1/q_m K_L \quad (3)$$

where Ce (mg/L) is an equilibrium concentration of dyes, q_e (mg/g) is the quantity of dye adsorbed on adsorbent at equilibrium, q_m (mg/g) is the maximum adsorbent capacity, and K_L (L/mg) is Langmuir constant. The isotherm plot between Ce/qe and Ce are shown in Fig. 10(a) [38].

The Freundlich adsorption isotherm is considered an empirical equation for a heterogeneous system in which multilayer adsorption may occur on the adsorbent surface. The equation of Freundlich isotherm is stated as follows Eq. (4) [16,57].

$$\mathrm{Log} q_e = \log K_f + 1/n \log C_e \quad (4)$$

In equation Ce (mg/L) is the equilibrium concentration of the dye solution, qe (mg/g) is the quantity of dye adsorbed at equilibrium, n determines the favorability of adsorption mechanism K_f is a Freundlich constant. The ln qe and ln Ce plots are shown in Fig. 10(b). The

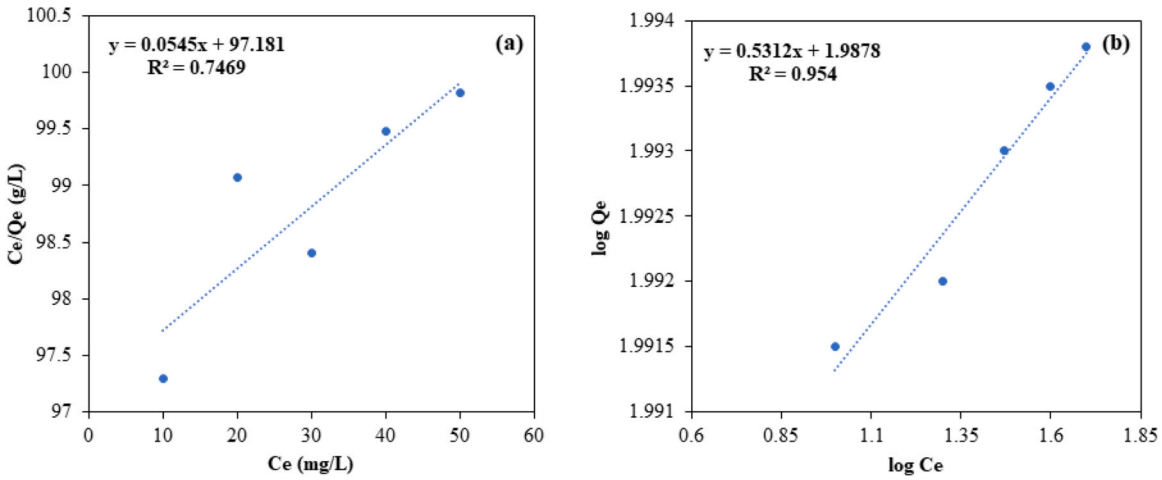

Fig. 10. Langmuir isotherm (a) and Freundlich isotherm (b) for methyl blue dye adsorption.

constraints of Langmuir and Freundlich equations from experimental data analysis are categorized in Table 2.

Usually, the estimation of the rectilinear regression correlation coefficient R^2 provides the signal which model can be best-fit. It identifies the difference between experimental and theoretical data as correlation coefficient value (R^2) approaches to 1. Based on the R^2 value of Langmuir and Freundlich models, it is observed that the attained experimentally data were fitted well by the Freundlich adsorption isotherm (R^2 = 0.954) than that of the Langmuir adsorption isotherm (R^2 = 0.746) (Table 2). This displays that the adsorption of MB dye on as-synthesized adsorbents (NS/TiO_2) was limited. Hence, the adsorbent surface was heterogeneous, which is a fair treaty with results described by Vimonses et al. [58]. The Freundlich isotherm constants, i.e., *Kf* and n are symbolic representations of the adsorption capacity and adsorbent intensity, respectively. The value of n for as-synthesized the adsorbent is 1.882 which is larger than unity and thus indicated that MB dye adsorption is favourable in this case. Furthermore, a more excellent value of n is the best signal of more potent adsorbate molecules bonding to the adsorbent surface. However, the high value of *Kf* point to adsorption capacity and higher affinity of MB dye to the adsorbent [53].

The adsorbent evaluated in this work showed a high *Kf* value, which indicates a high adsorption capacity. This increment in adsorption capacity can be attributed to large surface area and variation in particle size of adsorbent, which allows the dyes to get adsorbed on the adsorbent surface.

3.5. Kinetics and thermodynamics of NS/TiO_2 adsorbent

In order to evaluate the adsorption method in a more comprehensive way, the kinetic parameters of adsorption were designed. The analysis of mechanisms of adsorption has been done by means of the kinetic models including the pseudo first-order kinetic model and the pseudo second-order kinetic model.

The pseudo first-order equation is more appropriate for low concentration dye solution. It can be presented as following Eq. (5) [59]:

$$\ln (q_e - q_t) = \ln q_e - k_1 t \quad (5)$$

Table 2
Adsorption isotherm constants for MB adsorption onto NS co-doped TiO_2 for four hours.

Dye	Langmuir equation			Freundlich equation		
	R^2	Q_m	K_L (L/mg)	R^2	1/n (g/mg)	K_f (L/mg)
MB	0.746	0.054	97.18	0.954	1.882	1.97

Where k_1 (min^{-1}) is the rate constant for the pseudo first-order equation of adsorption, q_e and q_t (mg/g) is the quantity of MB adsorbed at time t and equilibrium. The values of k_1 and q_e were acquired from slopes and intercepts from the ln ($q_e - q_t$) and t plots as shown in Fig. 11(a).

The pseudo second-order equation is reliant on the quantity of the dye adsorbed on the adsorbent surface and the quantity adsorbed at the equilibrium. It can be denoted by the following Eq. (6) [60]:

$$t/q_t = 1/k_2 q_e^2 + t/q_e \quad (6)$$

Where k_2 (min^{-1}) is the rate constant for pseudo second-order adsorption equation, q_e and q_t (mg/g) is the quantity of MB adsorbed at time t and equilibrium. The values of k_2 and q_e are obtained from the slope and intercept of t/ q_t and t plot as shown in Fig. 11(b). The data for all the correlation coefficients (R^2) for pseudo first and second order equations is tabulated in Table 3. The values of R^2 for second-order equation is higher than all R^2 values of first-order equation which indicates that pseudo second-order model is more appropriate for elucidating the kinetics for MB adsorption onto NS/TiO_2. Similar outcomes have been testified for adsorption of MB onto graphene oxide/titania nanocomposites [38,61].

It is observed that maximum adsorption capacity for MB increases in range of 298–328 K by increasing the temperature (see Table 4.), which identifies an endothermic feature of existing process [38]. The thermodynamic parameters such as change in free energy ($\Delta\mathring{G}$), change in entropy ($\Delta\mathring{S}$) and change in enthalpy ($\Delta\mathring{H}$) are calculated from the intercept and slope of van't Hoff plots ($\ln k_L$ versus 1/T) using the Van't Hoff Eqs. (7–8):

$$\Delta\mathring{G} = -RT \ln k_L \quad (7)$$

$$\ln k_L = -\Delta\mathring{H}/RT + \Delta\mathring{S}/R \quad (8)$$

Where R (8.314 J mol^{-1} K^{-1}) is the general gas constant, k_L (L mol^{-1}) is the Langmuir constant and T (K) is the absolute temperature. The calculated $\Delta\mathring{S}$ is 185.96 ($J.mol^{-1}K^{-1}$) and the positive value relates to the increase in concentration of adsorbed species at solid/solution interface in the whole process of adsorption (Fig. 12). The calculated $\Delta\mathring{G}$ at different temperatures are −24.61, −25.12, −27.98 and −29.04 (kJ. mol^{-1}) and the negative values of $\Delta\mathring{G}$ recommends the spontaneity and feasibility of adsorption method. Finally, the intended $\Delta\mathring{H}$ (32.34 kJ. mol^{-1}) determines an endothermic adsorption process in agreement with increase in adsorption capacity with increasing temperature [62].

3.6. Adsorption mechanism

Interactions that occur between the adsorbate and adsorbent molecules can manifest themselves in various ways [63]. Hypothetical

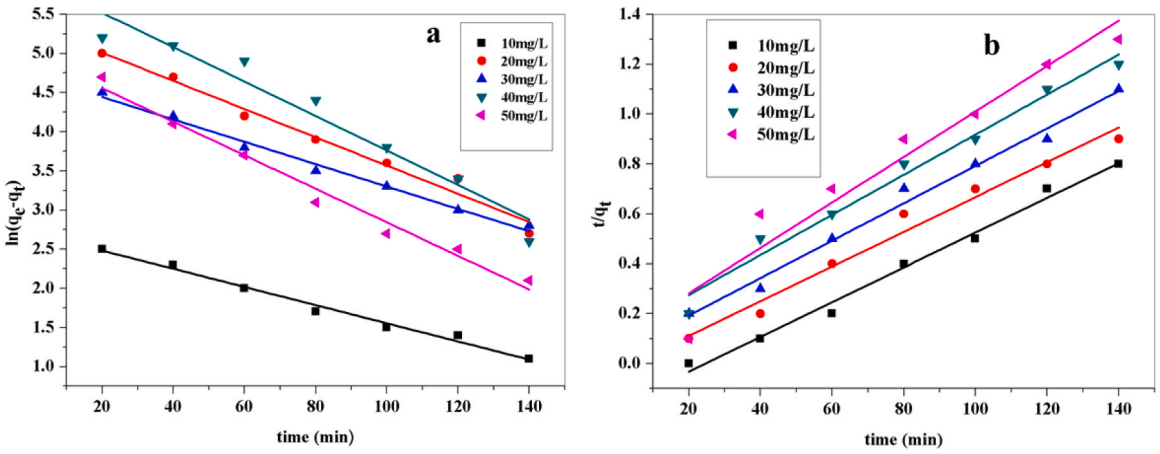

Fig. 11. Plots of pseudo-first-order model (a) and pseudo-second-order model (b) for the adsorption MB onto NS/TiO_2.

Table 3
Kinetic parameters for the adsorption of MB.

C_e (mg/L)	First order-kinetics		Second order-kinetics	
	k_1 (min^{-1})	R^2	k_2 (min^{-1})	R^2
10	0.0436	0.97904	0.0325	0.98112
20	0.0421	0.93752	0.0113	0.97733
30	0.0283	0.98612	0.0016	0.98855
40	0.0253	0.97704	0.0011	0.98739
50	0.0211	0.98458	0.0004	0.98923

Table 4
Thermodynamic parameters for MB adsorption on NS/TiO_2.

Temp (K)	$\Delta\mathring{G}$ (kJ.mol^{-1})	$\Delta\mathring{S}$ (J.$mol^{-1}K^{-1}$)	$\Delta\mathring{H}$ (kJ.mol^{-1})
298	-24.61		
308	-25.12	185.96	32.34
318	-27.98		
328	-29.04		

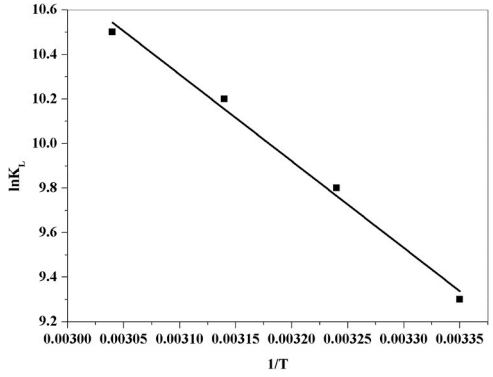

Fig. 12. Plot of ln K_L versus 1/T for the adsorption of MB onto NS/TiO_2.

treatments of adsorbate-adsorbent connections, beginning with Grimley and co-workers [64], Einstein and Schrieffer [65], have focused on the indirect attraction through the surface electrons. For the large adsorbate-adsorbent partition, this collaboration is oscillatory in sign and magnitude. Recently, Joyner et al. [66] and Feibelman et al. [67] determined the change in surface electron-density due to electronegative or electropositive atom adsorption. Such changes are accepted to influence the connection of an adsorbing molecule with the surface. The immediate interaction due to the overlapping of orbitals between different adsorbate and adsorbent molecules have also been studied [68, 69]. The dye adsorption process from the aqueous solution onto the porous adsorbent surface involves different mechanisms, including functional groups on the surface of the adsorbent, active sites, and the adsorbent charges.

The adsorption of contaminants or dye to the adsorbent surface is carried out by electrostatic interactions of surface charges and hydrogen bonding. N and S doping on TiO_2 provides more active sites for interaction with dye molecules, as shown in Fig. 13. N is doped at the interstitial site of oxygen and S is doped at the titania site in the form of SO_4^{-2} ions. As a result of electrostatic interactions and hydrogen bonding (physical forces), the dye molecules (MB) adsorb on the surface of NS/TiO_2, thus involved in removing dyes from the solution. Table 5. Summarize the comparison of removal effeciency by different adsorbents.

3.7. *Recovery and reusability of adsorbent*

For large scope wastewater treatment, adsorbent ought to have properties like high adsorption capacity, high stability and easy separation from dye solution after adsorption. To make the adsorption process economical, regeneration and reusability of adsorbent are significant. Abramian et al. described in their investigation the removal of methylene blue by highly porous titania aerogel and had shown the results of adsorption-desorption for three runs [73].

The adsorption capacity of regenerated NS/TiO_2 in the second and third run was tested under acidic medium for MB solution and basic medium for MO and MR dye solutions. The obtained results are compared with the first run, as shown in Fig. 14. The uptake limit of reused adsorbent showed a magnificent adsorption capacity compared to the first cycle of adsorption. The approx. 90%, 70% and 68% removal was obtained for the second run and 70%, 50% and 39% removal was obtained for the third run compared to the first cycle where 99.4%, 98% and 96% removal was obtained for MB, MO, and MR, respectively.

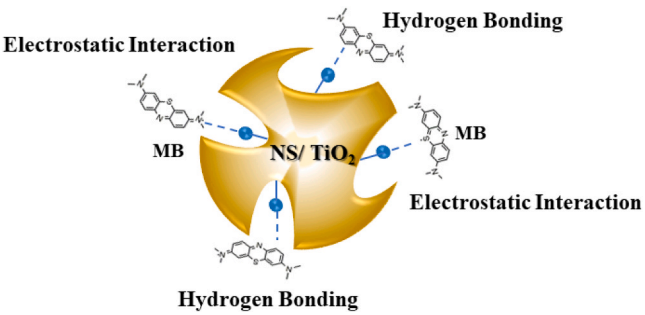

Fig. 13. Pictographic representation and the adsorption mechanism of methylene blue.

Table 5
Comparison of removal effeciency by different adsorbents.

Adsorbent	Time (min)	Removal efficiency (%)	References
TiO_2	45	5	[70]
N-doped TiO_2	240	76	[71]
S-doped TiO_2		72.1	[72]
NS/TiO_2	120	99.4	This work

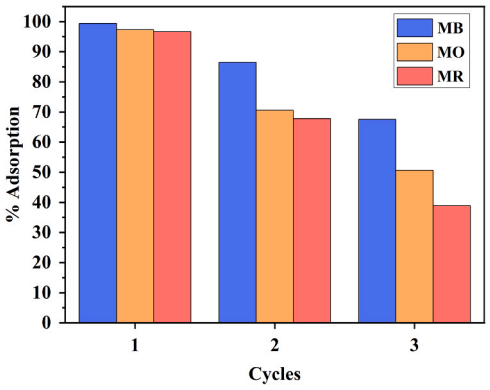

Fig. 14. Regeneration and recyclability of the as-synthesized NS/TiO_2.

Hence a decline in initial adsorption capacity is observed with the number of cycles. However, nearly 99.4% of the initial dye concentration was adsorbed on as-synthesized NS/TiO_2 after 100 min of contact between the solid-liquid interface for the three compared cycles.

4. Conclusion

The paper examines the adsorption of dyes such as MB, MO and MR on the NS co-doped titania. Doping of TiO_2 with nitrogen and sulfur provides a large surface area, porous structure and more electrostatic binding sites for the adsorption of dyes, specifically for MB. The parametric study showed that NS/TiO_2 exhibited the highest adsorption capacity for MB that was 99.4%, compared to other dyes. The adsorption of MB on NS/TiO_2 adsorbent was investigated by different parameters, including pH, initial dye concentration, adsorbent dose and contact time. The experimental data is the best fit for Freundlich isotherm, revealing that heterogeneous adsorbent surfaces provide the maximum adsorption to remove dyes. The dye desorption from NS/TiO_2 adsorbent for regeneration purposes could be carried out in an acidic medium. The dye retaining system is mainly due to electrostatic interactions of dye molecules with the adsorbent surface. The presented study concludes that NS/TiO_2 could be used as an effective adsorbent, especially for cationic dyes with low concentration in the process of wastewater treatment. NS/TiO_2 adsorbent is efficient and can be used for the removal of pollutants at commercial scale in the future because of its promising benefits. Considering the financial aspect of adsorbent, it shows low operational and characterization costs and high adsorption capacity.

Even though the number of researches have published on adsorbents for pollutants and dye removal, there is yet little work has done for the commercial applications of adsorbents. In addition, associations of different adsorbents are problematic because of discrepancies in the data management. Thus, extensive work is required to better recognize adsorption process and to establish the potential technology at industrial scale.

CRediT authorship contribution statement

Ruhma Rashid: Data curation, Formal analysis, Investigation, Writing - original draft. **Iqrash Shafiq:** Data curation, Formal analysis, Investigation, Writing - original draft. **Muhammad Javid Iqbal:** Conceptualization, Methodology, Project administration, Resources, Supervision. **Maira Shabir:** Data curation, Formal analysis, Investigation, Writing - review & editing. **Parveen Akhter:** Conceptualization, Methodology, Project administration, Validation, Resources, Writing - review & editing. **Muhammad Haris Hamayun:** Data curation, Formal analysis, Software, Investigation, Writing - review & editing. **Ashfaq Ahmed:** Conceptualization, Project administration, Resources, Validation, Writing - review & editing. **Murid Hussain:** Conceptualization, Methodology, Project administration, Resources, Supervision, Validation, Visualization, Funding acquisition, Writing - review & editing.

Declaration of Competing Interest

The authors declare that they have no known competing financial interests or personal relationships that could have appeared to influence the work reported in this paper.

Acknowledgement

Dr. M. Hussain would like to thank the Higher Education Commission (HEC), Pakistan, for the funding under TDF Project (TDF02-011).

References

[1] A.A. Scharnberg, A.C. de Loreto, A.K. Alves, Optical and structural characterization of $Bi_2Fe_xNbO_7$ nanoparticles for environmental applications, Emerg. Sci. J. 4 (1) (2020) 11–17, https://doi.org/10.28991/esj-2020-01205.
[2] I. Shafiq, S. Shafique, P. Akhter, G. Abbas, A. Qurashi, M. Hussain, Efficient catalyst development for deep aerobic photocatalytic oxidative desulfurization: recent advances, confines, and outlooks, Catal. Rev. (2021) 1–46, https://doi.org/10.1080/01614940.2020.1864859.
[3] I. Shafiq, et al., Recent breakthroughs in deep aerobic oxidative desulfurization of petroleum refinery products, J. Clean. Prod. (2020), 125731, https://doi.org/10.1016/j.jclepro.2020.125731.
[4] I. Shafiq, S. Shafique, P. Akhter, W. Yang, M. Hussain, Recent developments in alumina supported hydrodesulfurization catalysts for the production of sulfur-free refinery products: a technical review, Catal. Rev. (2020) 1–86, https://doi.org/10.1080/01614940.2020.1780824.
[5] X. Zhao, H. Chen, F. Kong, Y. Zhang, S. Wang, S. Liu, L.A. Lucia, P. Fatehi, H. Pang, Fabrication, characteristics and applications of carbon materials with different morphologies and porous structures produced from wood liquefaction: a review, Chem. Eng. J. 364 (2019) 226–243, https://doi.org/10.1016/j.cej.2019.01.159.
[6] I.M. Kolangare, A.M. Isloor, Inamuddin, A.M. Asiri, A.F. Ismail, Improved desalination by polyamide membranes containing hydrophilic glutamine and glycine, Environ. Chem. Lett. 17 (2) (2019) 1053–1059, https://doi.org/10.1007/s10311-018-00825-1.
[7] R. Ansari, M.B. Keivani, A.F. Delavar, Application of polypyrrole coated onto wood sawdust for the removal of carmoisine dye from aqueous solutions, J. Appl. Polym. Sci. 122 (2) (2011) 804–812, https://doi.org/10.1002/app.34051.
[8] A. Ali, N. Ejaz, S. Nasreen, A. Nasir, L.A. Qureshi, B.M. Al-Sakkaf, Enhanced degradation of dyes present in textile effluent by ultrasound assisted electrochemical reactor, Civ. Eng. J. 5 (10) (2019) 2131–2142, https://doi.org/10.28991/cej-2019-03091399.
[9] I. Shafiq, M. Hussain, N. Shehzad, I.M. Maafa, P. Akhter, U. Amjad, S. Shafique, A. Razzaq, W. Yang, M. Tahir, N. Russo, The effect of crystal facets and induced porosity on the performance of monoclinic $BiVO_4$ for the enhanced visible-light driven photocatalytic abatement of methylene blue, J. Environ. Chem. Eng. 7 (4) (2019), 103265, https://doi.org/10.1016/j.jece.2019.103265.
[10] K. Azam, R. Raza, N. Shezad, M. Shabir, W. Yang, N. Ahmad, I. Shafiq, P. Akhter, A. Razzaq, M. Hussain, Development of recoverable magnetic mesoporous carbon adsorbent for removal of methyl blue and methyl orange from wastewater, J. Environ. Chem. Eng. 8 (5) (2020), 104220, https://doi.org/10.1016/j.jece.2020.104220.
[11] T.K. Sen, S. Afroze, H. Ang, Equilibrium, kinetics and mechanism of removal of methylene blue from aqueous solution by adsorption onto pine cone biomass of Pinus radiata, Water Air Soil Pollut. 218 (1–4) (2011) 499–515, https://doi.org/10.1007/s11270-010-0663-y.
[12] M.T. Yagub, T.K. Sen, H. Ang, Equilibrium, kinetics, and thermodynamics of methylene blue adsorption by pine tree leaves, Water Air Soil Pollut. 223 (8) (2012) 5267–5282, https://doi.org/10.1007/s11270-012-1277-3.
[13] M. Abbas, Experimental investigation of titanium dioxide as an adsorbent for removal of Congo red from aqueous solution, equilibrium and kinetics modeling, J. Water Reuse Desalin. 10 (3) (2020) 251–266, https://doi.org/10.2166/wrd.2020.038.
[14] V. Gupta, Application of low-cost adsorbents for dye removal–a review, J. Environ. Manag. 90 (8) (2009) 2313–2342, https://doi.org/10.1016/j.jenvman.2008.11.017.

[15] Z.A. Bhatti, K. Qureshi, G. Maitlo, S. Ahmed, Study of PAN fiber and iron ore adsorbents for arsenic removal, Civ. Eng. J. 6 (3) (2020) 548–562, https://doi.org/10.28991/cej-2020-03091491.

[16] S. Chahid, R. Alcántara, D.M. los Santos, Isotherm analysis for removal of organic pollutants Using Synthesized Mo/Cu/co-doped TiO2 Nanostrucrured, in: Proceedings of the 2019 5th International Conference on Optimization and Applications (ICOA) 2019 IEEE, doi: 10.1109/ICOA.2019.8727623.

[17] F. Mashkoor, A. Nasar, Carbon nanotube-based adsorbents for the removal of dyes from waters: a review, Environ. Chem. Lett. (2020) 1–25, https://doi.org/10.1007/s10311-020-00970-6.

[18] Z. Jiang, M. Chen, J. Shi, J. Yuan, W. Shangguan, Catalysis removal of indoor volatile organic compounds in room temperature: from photocatalysis to active species assistance catalysis, Catal. Surv. Asia 19 (1) (2015) 1–16, https://doi.org/10.1007/s10563-014-9177-8.

[19] A. Doner, Comparison of corrosion behaviors of bare Ti and TiO_2, Emerg. Sci. J. 3 (4) (2019) 235–240, https://doi.org/10.28991/esj-2019-01185.

[20] E.C. Lima, Removal of emerging contaminants from the environment by adsorption, Ecotoxicol. Environ. Saf. 150 (2018) 1–17, https://doi.org/10.1016/j.ecoenv.2017.12.026.

[21] N. Tara, S.I. Siddiqui, G. Rathi, S.A. Chaudhry, Inamuddin, A.M. Asiri, Nano-engineered adsorbent for the removal of dyes from water: a review, Curr. Anal. Chem. 16 (1) (2020) 14–40, https://doi.org/10.2174/1573411015666190117124344.

[22] M. Buaisha, S. Balku, S. Özalp-Yaman, Heavy metal removal investigation in conventional activated sludge systems, Civ. Eng. J. 6 (3) (2020) 470–477, https://doi.org/10.28991/cej-2020-03091484.

[23] J. Tian, J. Xu, F. Zhu, T. Lu, C. Su, G. Ouyang, Application of nanomaterials in sample preparation, J. Chromatogr. A 1300 (2013) 2–16, https://doi.org/10.1016/j.chroma.2013.04.010.

[24] I.M. El-Nahhal, et al., Nano-structured zinc oxide–cotton fibers: synthesis, characterization and applications, J. Mater. Sci.: Mater. Electron. 24 (10) (2013) 3970–3975, https://doi.org/10.1007/s10854-013-1349-1.

[25] X.M. Yan, B.Y. Shi, J.J. Lu, C.H. Feng, D.S. Wang, H.X. Tang, Adsorption and desorption of atrazine on carbon nanotubes, J. Colloid Interface Sci. 321 (1) (2008) 30–38, https://doi.org/10.1016/j.jcis.2008.01.047.

[26] A.A. Vega, G.E. Imoberdorf, M. Mohseni, Photocatalytic degradation of 2, 4-dichlorophenoxyacetic acid in a fluidized bed photoreactor with composite template-free TiO_2 photocatalyst, Appl. Catal. A: Gen. 405 (1–2) (2011) 120–128, https://doi.org/10.1016/j.apcata.2011.07.033.

[27] S. Helali, E. Puzenat, N. Perol, M.J. Safi, C. Guillard, Methylamine and dimethylamine photocatalytic degradation—Adsorption isotherms and kinetics, Appl. Catal. A: Gen. 402 (1–2) (2011) 201–207, https://doi.org/10.1016/j.apcata.2011.06.004.

[28] M. Ashida, M. Sasaki, H. Kan, T. Yasunaga, K. Hachiya, T. Inoue, Kinetics of proton adsorption-desorption at TiO_2-H_2O interface by means of pressure-jump technique, J. Colloid Interface Sci. 67 (2) (1978) 219–225, https://doi.org/10.1016/0021-9797(78)90005-X.

[29] A. Döner, Comparison of corrosion behaviors of bare Ti and TiO_2, Emerg. Sci. J. 3 (4) (2019) 235–240, https://doi.org/10.28991/esj-2019-01185.

[30] P. Akhter, M. Hussain, G. Saracco, N. Russo, Novel nanostructured-TiO_2 materials for the photocatalytic reduction of CO_2 greenhouse gas to hydrocarbons and syngas, Fuel 149 (2015) 55–65, https://doi.org/10.1016/j.fuel.2014.09.079.

[31] M. Hussain, P. Akhter, N. Russo, G. Saracco, Novel Ti-KIT-6 material for the photocatalytic reduction of carbon dioxide to methane, Catal. Commun. 36 (2013) 58–62, https://doi.org/10.1016/j.catcom.2013.03.002.

[32] U. Baig, M.K. Uddin, M. Sajid, Surface modification of TiO_2 nanoparticles using conducting polymer coating: spectroscopic, structural, morphological characterization and interaction with dye molecules, Mater. Today Commun. 25 (2020), 101534, https://doi.org/10.1016/j.mtcomm.2020.101534.

[33] W.-C. Hung, S.H. Fu, J.J. Tseng, H. Chu, T.H. Ko, Study on photocatalytic degradation of gaseous dichloromethane using pure and iron ion-doped TiO_2 prepared by the sol–gel method, Chemosphere 66 (11) (2007) 2142–2151, https://doi.org/10.1016/j.chemosphere.2006.09.037.

[34] K. Pelentridou, E. Stathatos, H. Karasali, D.D. Dionysiou, P. Lianos, Photocatalytic degradation of a water soluble herbicide by pure and noble metal deposited TiO_2 nanocrystalline films, Int. J. Photoenergy 2008 (2008) 1–7, https://doi.org/10.1155/2008/978329.

[35] R.S. Raveendra, P.A. Prashanth, R. Hari Krishna, N.P. Bhagya, B.M. Nagabhushana, H. Raja Naika, K. Lingaraju, H. Nagabhushana, B. Daruka Prasad, Synthesis, structural characterization of nano $ZnTiO_3$ ceramic: an effective azo dye adsorbent and antibacterial agent, J. Asian Ceram. Soc. 2 (4) (2014) 357–365, https://doi.org/10.1016/j.jascer.2014.07.008.

[36] Y. Zhao, X. Li, C. Tian, J. Wang, Production of carbon-doped titanium dioxide (C–TiO_2) from polytitanium-coagulated sludge as an adsorbent or photocatalyst for pollutant removals, J. Clean. Prod. 267 (2020), 121979, https://doi.org/10.1016/j.jclepro.2020.121979.

[37] M. Ksibi, S. Rossignol, J.M. Tatibouët, C. Trapalis, Synthesis and solid characterization of nitrogen and sulfur-doped TiO_2 photocatalysts active under near visible light, Mater. Lett. 62 (26) (2008) 4204–4206, https://doi.org/10.1016/j.matlet.2008.06.026.

[38] H. Wang, H. Gao, M. Chen, X. Xu, X. Wang, C. Pan, J. Gao, Microwave-assisted synthesis of reduced graphene oxide/titania nanocomposites as an adsorbent for methylene blue adsorption, Appl. Surf. Sci. 360 (2016) 840–848, https://doi.org/10.1016/j.apsusc.2015.11.075.

[39] M. Naushad, A.A. Alqadami, Z.A. AlOthman, I.H. Alsohaimi, M.S. Algamdi, A. M. Aldawsari, Adsorption kinetics, isotherm and reusability studies for the removal of cationic dye from aqueous medium using arginine modified activated carbon, J. Mol. Liq. 293 (2019), 111442, https://doi.org/10.1016/j.molliq.2019.111442.

[40] G. Liu, C. Sun, S.C. Smith, L. Wang, G.Q. Lu, H.M. Cheng, Sulfur doped anatase TiO_2 single crystals with a high percentage of {0 0 1} facets, J. Colloid Interface Sci. 349 (2) (2010) 477–483, https://doi.org/10.1016/j.jcis.2010.05.076.

[41] Y.-H. Lin, C.H. Weng, A.L. Srivastav, Y.T. Lin, J.H. Tzeng, Facile synthesis and characterization of N-doped TiO_2 photocatalyst and its visible-light activity for photo-oxidation of ethylene, J. Nanomater. 2015 (2015) 1–10, https://doi.org/10.1155/2015/807394.

[42] H. Lin, C. Huang, W. Li, C. Ni, S. Shah, Y. Tseng, Size dependency of nanocrystalline TiO_2 on its optical property and photocatalytic reactivity exemplified by 2-chlorophenol, Appl. Catal. B: Environ. 68 (1–2) (2006) 1–11, https://doi.org/10.1016/j.apcatb.2006.07.018.

[43] A.J. Albrbar, V. Djokić, A. Bjelajac, J. Kovač, J. Ćirković, M. Mitrić, D. Janaćković, R. Petrović, Visible-light active mesoporous, nanocrystalline N, S-doped and co-doped titania photocatalysts synthesized by non-hydrolytic sol-gel route, Ceram. Int. 42 (15) (2016) 16718–16728, https://doi.org/10.5402/2011/261219.

[44] L. Zou, Y. Luo, M. Hooper, E. Hu, Removal of VOCs by photocatalysis process using adsorption enhanced TiO_2–SiO_2 catalyst, Chem. Eng. Process.: Process Intensif. 45 (11) (2006) 959–964, https://doi.org/10.1016/j.cep.2006.01.014.

[45] M. Hussain, R. Ceccarelli, D.L. Marchisio, D. Fino, N. Russo, F. Geobaldo, Synthesis, characterization, and photocatalytic application of novel TiO_2 nanoparticles, Chem. Eng. J. 157 (1) (2010) 45–51, https://doi.org/10.1016/j.cej.2009.10.043.

[46] D.S. Bhatkhande, V.G. Pangarkar, A.A.C.M. Beenackers, Photocatalytic degradation for environmental applications–a review, J. Chem. Technol. Biotechnol.: Int. Res. Process Environ. Clean. Technol. 77 (1) (2002) 102–116, https://doi.org/10.1002/jctb.532.

[47] M. Al-Amin, et al., Solar assisted photocatalytic degradation of reactive azo dyes in presence of anatase titanium dioxide, Int. J. Latest Res. Eng. Technol. 2 (3) (2016) 14–21.

[48] M.S. Azami, W.I. Nawawi, A.H. Jawad, M.A.M. Ishak, K. Ismail, N-doped TiO_2 synthesised via microwave induced photocatalytic on RR4 dye removal under LED light irradiation, Sains Malays. 46 (8) (2017) 1309–1316, https://doi.org/10.17576/jsm-2017-4608-17.

[49] L.G. Devi, R. Kavitha, Enhanced photocatalytic activity of sulfur doped TiO_2 for the decomposition of phenol: a new insight into the bulk and surface modification, Mater. Chem. Phys. 143 (3) (2014) 1300–1308, https://doi.org/10.1016/j.matchemphys.2013.11.038.

[50] M. Estrada, C. Reza, J. Salmones, J.A. Wang, M.E. Manríquez, J.M. Mora, M. L. Hernández, A. Zúñiga, J.L. Contreras, Synthesis of nanoporous TiO_2 thin films for photocatalytic degradation of methylene blue, JNMES 17 (1) (2014) 023–028, https://doi.org/10.14447/jnmes.v17i1.439.

[51] X. Cheng, X. Yu, Z. Xing, L. Yang, Synthesis and characterization of N-doped TiO_2 and its enhanced visible-light photocatalytic activity, Arab. J. Chem. 9 (2016) S1706–S1711, https://doi.org/10.1016/j.arabjc.2012.04.052.

[52] N. Li, X. Zhang, W. Zhou, Z. Liu, G. Xie, Y. Wang, Y. Du, High quality sulfur-doped titanium dioxide nanocatalysts with visible light photocatalytic activity from non-hydrolytic thermolysis synthesis, Inorg. Chem. Front. 1 (7) (2014) 521–525, https://doi.org/10.1039/C4QI00027G.

[53] B. Tanhaei, A. Ayati, M. Lahtinen, M. Sillanpää, Preparation and characterization of a novel chitosan/Al_2O_3/magnetite nanoparticles composite adsorbent for kinetic, thermodynamic and isotherm studies of Methyl Orange adsorption, Chem. Eng. J. 259 (2015) 1–10, https://doi.org/10.1016/j.cej.2014.07.109.

[54] B. Ramaraju, P. Manoj Kumar Reddy, C. Subrahmanyam, Low cost adsorbents from agricultural waste for removal of dyes, Environ. Prog. Sustain. Energy 33 (1) (2014) 38–46, https://doi.org/10.1002/ep.11742.

[55] S. Tahir, N. Rauf, Removal of a cationic dye from aqueous solutions by adsorption onto bentonite clay, Chemosphere 63 (11) (2006) 1842–1848, https://doi.org/10.1016/j.chemosphere.2005.10.033.

[56] K.-H. Park, T.Y. Kim, J.Y. Park, E.M. Jin, S.H. Yim, D.Y. Choi, J.W. Lee, Adsorption characteristics of gardenia yellow as natural photosensitizer for dye-sensitized solar cells, Dyes Pigments 96 (2) (2013) 595–601, https://doi.org/10.1016/j.dyepig.2012.10.005.

[57] S. Li, Removal of crystal violet from aqueous solution by sorption into semi-interpenetrated networks hydrogels constituted of poly (acrylic acid-acrylamide-methacrylate) and amylose, Bioresour. Technol. 101 (7) (2010) 2197–2202, https://doi.org/10.1016/j.biortech.2009.11.044.

[58] V. Vimonses, S. Lei, B. Jin, C.W.K. Chow, C. Saint, Kinetic study and equilibrium isotherm analysis of Congo Red adsorption by clay materials, Chem. Eng. J. 148 (2–3) (2009) 354–364, https://doi.org/10.1016/j.cej.2008.09.009.

[59] M. Doğan, Y. Özdemir, M. Alkan, Adsorption kinetics and mechanism of cationic methyl violet and methylene blue dyes onto sepiolite, Dyes Pigments 75 (3) (2007) 701–713, https://doi.org/10.1016/j.dyepig.2006.07.023.

[60] K.G. Bhattacharyya, S.S. Gupta, Kaolinite, montmorillonite, and their modified derivatives as adsorbents for removal of Cu (II) from aqueous solution, Sep. Purif. Technol. 50 (3) (2006) 388–397, https://doi.org/10.1016/j.seppur.2005.12.014.

[61] X. Liu, S. Huang, Y. Su, Z. Chai, H. Zhai, X. Wang, A novel adsorbent of $Na_2Ta_2O_6$ porous microspheres with F− gradient concentration distribution: high cationic selectivity and well-regulated recycling, J. Hazard. Mater. 265 (2014) 226–232, https://doi.org/10.1016/j.jhazmat.2013.11.062.

[62] D. Wang, L. Liu, X. Jiang, J. Yu, X. Chen, X. Chen, Adsorbent for p-phenylenediamine adsorption and removal based on graphene oxide functionalized with magnetic cyclodextrin, Appl. Surf. Sci. 329 (2015) 197–205, https://doi.org/10.1016/j.apsusc.2014.12.161.

[63] N. Lang, S. Holloway, J. Nørskov, Electrostatic adsorbate-adsorbate interactions: the poisoning and promotion of the molecular adsorption reaction, Surf. Sci. 150 (1) (1985) 24–38, https://doi.org/10.1016/0039-6028(85)90208-0.
[64] T. Grimley, S. Walker, Interactions between adatoms on metals and their effects on the heat of adsorption at low surface coverage, Surf. Sci. 14 (2) (1969) 395–406, https://doi.org/10.1016/0039-6028(69)90087-9.
[65] T. Einstein, J. Schrieffer, Indirect interaction between adatoms on a tight-binding solid, Phys. Rev. B 7 (8) (1973) 3629–3648, https://doi.org/10.1103/PhysRevB.7.3629.
[66] R.W. Joyner, J.B. Pendry, D.K. Saldin, S.R. Tennison, Metal-support interactions in heterogeneous catalysis, Surf. Sci. 138 (1) (1984) 84–94, https://doi.org/10.1016/0039-6028(84)90497-7.
[67] P.J. Feibelman, D. Hamann, Electronic structure of a“ poisoned” transition-metal surface, Phys. Rev. Lett. 52 (1) (1984) 61–64, https://doi.org/10.1103/PhysRevLett.52.61.
[68] Y. Muda, T. Hanawa, Study of adsorption by the extended Hückel theory: CO on diamond (111) surface, Jpn. J. Appl. Phys. 13 (6) (1974) 930–932, https://doi.org/10.1143/JJAP.13.
[69] J. Benziger, R. Madix, The effects of carbon, oxygen, sulfur and potassium adlayers on CO and H_2 adsorption on Fe (100), Surf. Sci. 94 (1) (1980) 119–153, https://doi.org/10.1016/0039-6028(80)90160-0.
[70] D. Maučec, A. Šuligoj, A. Ristić, G. Dražić, A. Pintar, N.N. Tušar, Titania versus zinc oxide nanoparticles on mesoporous silica supports as photocatalysts for removal of dyes from wastewater at neutral pH, Catal. Today 310 (2018) 32–41, https://doi.org/10.1016/j.cattod.2017.05.061.
[71] P. Mehdizadeh, et al., Visible light activity of nitrogen-doped TiO_2 by sol-gel method using various nitrogen sources, J. Nanostruct. 10 (2) (2020) 307–316, https://doi.org/10.22052/JNS.2020.02.010.
[72] R.T. Bento, O.V. Correa, M.F. Pillis, On the surface chemistry and the reuse of sulfur-doped TiO_2 films as photocatalysts, Mater. Chem. Phys. 261 (2021), 124231, https://doi.org/10.1016/j.matchemphys.2021.124231.
[73] L. Abramian, H. El-Rassy, Adsorption kinetics and thermodynamics of azo-dye Orange II onto highly porous titania aerogel, Chem. Eng. J. 150 (2–3) (2009) 403–410, https://doi.org/10.1016/j.cej.2009.01.019.